RAPID COMMUNICATIONS

PHYSICAL REVIEW B VOLUME 46, NUMBER 19 15 NOVEMBER 1992-I

Weak localization in short one-dimensional channels contacted by two-dimensional probes

C. de Graaf,* J. Caro, and S. Radelaar

Delft Institute of Microelectronics and Submicron Technology, Delft University of Technology, Lorentzweg 1, 2628 CJ Delft, The Netherlands

(Received 8 September 1992)

In this paper we show that the low-field magnetoconductance of a short one-dimensional channel contacted by two-dimensional probes in a silicon MOSFET can be described by a recent theory, which includes the influence of the probes on the magnitude and shape of the weak-localization correction as a function of magnetic field. The temperature dependence of the phase-coherence length indicates that, in the investigated range of temperatures, electron-electron scattering involving large energy transfers is the dominant phase-breaking mechanism.

Contemporary nanolithographic technologies allow the fabrication of one-dimensional wires of length L comparable to or even much shorter than the phase-coherence length l_ϕ. For instance, in silicon metal-oxide-semiconductor field-effect transistors (MOSFET's) l_ϕ is about 500 nm at 1 K, whereas structures smaller than 100 nm can easily be made. In metals it is usually even easier to reach the limit $L \ll l_\phi$. The standard theoretical expressions[1,2] for the low-field magnetoconductance (LFMC) due to weak localization usually fit excellently to experimental data for two-dimensional (2D) or *long* 1D systems, because contributions to the magnetoconductance arising from other effects like electron-electron interaction and the classical magnetoconductance are negligible in the weak-localization regime.[3] Therefore, LFMC experiments are widely used to determine l_ϕ.

It was found, however, that l_ϕ, as inferred from fits of the standard weak-localization formula to LFMC experiments on very *short* wires of length $L \lesssim l_\phi$, is shorter than values obtained for longer wires and 2D films of the same material.[4] This can be understood from the fact that if $L \lesssim l_\phi$, the time-reversed scattering paths[5] leading to weak localization extend into the probes. Since the magnitude of the weak-localization correction δG depends on the return probability of electrons, and since this return probability will be smaller if the region to which an electron can travel within a time $\tau_\phi \propto l_\phi^2$ is larger, wide probes will lead to a δG smaller than expected from the standard formula. Recently, Chandrasekhar *et al.*[4,6] extended the theory of weak localization to include the geometry of the probes. They showed that both the magnitude of δG and the shape of the LFMC curves are affected by the probes, and found excellent agreement between the theory and experiments on short silver wires. The theory has also been applied to metal rings,[7] but as far as we know, the present paper discusses the first experiments in which their expression for the low-field magnetoconductance is tested on small *semiconducting* systems.

The devices used in our experiments are dual-gate silicon MOSFET's, in which a short 1D channel can be induced by applying a negative voltage V_{GL} to the lower split gate. A positive voltage V_{GU} on the upper gate induces the electron gas in the 2D areas on both sides of the split gate and in the 1D channel. A top view of the device is shown in Fig. 1. The width of the gap in the split gate is 350 nm but due to fringing fields the width W of the conducting 1D channel between the two large 2D contact areas can be much smaller. In one of the devices (No. 1) the length of the split gate was 730 nm, and in another (No. 2) it was 90 nm. The real 1D channel length L will be larger, which is again the result of the fringing field of the lower gate. Also, the bottom of the conduction band in the 1D channel will lie at a higher energy than in the 2D regions. Since l_ϕ depends via the diffusion constant on the electron concentration, the values of $l_{\phi,1D}$ and $l_{\phi,2D}$ in the 1D channel and 2D regions are not necessarily equal.

The low-field magnetoconductance of the devices was measured using a standard four-probe ac lock-in technique. In essence, however, the measurement of the conductance of the 1D channel is two probe, because the channel conductance is much lower than that of the 2D regions, which act as contacts. Figure 2 shows a low-field magnetoconductance curve for device No. 1 at $T = 1200$ mK and constant $V_{GU} = 15$ V and $V_{GL} = -7.5$ V. The

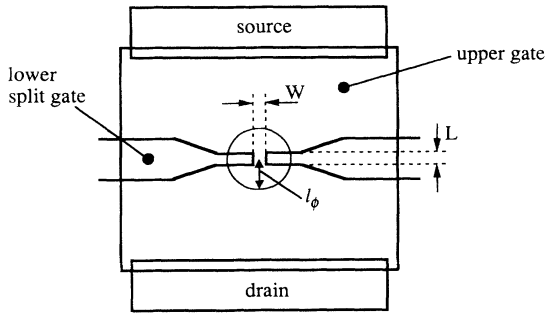

FIG. 1. Schematic drawing of the MOSFET used in the experiments. A lower split gate with a gap of length $L \lesssim l_\phi$ and width $W \ll l_\phi$ defines a narrow channel between the two large two-dimensional electron gases induced by the upper gate. Electrons starting in the narrow channel can diffuse to the area indicated by the circle without losing phase coherence.

strong dip in the conductance G around zero field is due to weak localization, whereas universal conductance fluctuations are clearly present at higher fields. In Fig. 3 an enlarged view of the region around zero field is given, at a number of different temperatures. A similar set of data was obtained for device No. 2.

We fitted the standard 1D weak-localization formula[1]

$$\delta G_1(B) = -\frac{g_v \alpha e^2}{\pi \hbar L}\left[\frac{1}{l_\phi^2}+\frac{W^2}{12 l_B^4}\right]^{-1/2}, \quad (1)$$

the standard 2D formula[2],

$$\delta G_2(B) = -\frac{g_v \alpha e^2 W}{2\pi^2 \hbar L}\left[\Psi\left[\frac{1}{2}+\frac{\hbar}{4eBl_\phi^2}\right] - \Psi\left[\frac{1}{2}+\frac{\hbar}{4eBl_e^2}\right]\right], \quad (2)$$

and Chandrasekhar's formula for the case of a 1D channel contacted by two 2D half-planes:[6]

$$\delta G_{1D\text{-}2D}(B) = -\frac{g_v \alpha e^2}{\pi \hbar}\frac{l_{\phi,1D}}{L}\left[\frac{(\eta^2+\beta^2)\coth(L/l_{\phi,1D}) - (l_{\phi,1D}/L)(\eta^2-\beta^2)+2\eta\beta}{\eta^2+\beta^2+2\eta\beta\coth(L/l_{\phi,1D})}\right] \quad (3)$$

to all LFMC curves of Fig. 3. In these formulas g_v is the valley degeneracy, which equals 2 in (100) silicon MOSFET's and the factor α describes intervalley scattering. $l_B = (\hbar/2eB)^{1/2}$ is the magnetic length and l_e the elastic scattering length, which in our silicon MOSFET's is about 50 nm. In Eq. (3) $\beta(B) = W/l_{\phi,1D}(B)$ and $l_{\phi,1D}(B) = (l_{\phi,1D}^{-2} + W^2/12 l_B^4)^{-1/2}$. η is given by

$$\eta(B=0) = \frac{\pi}{\ln(l_{\phi,2D}/l_e)},$$
$$\eta(B\neq 0) = \frac{-2\pi}{\Psi\left[\frac{1}{2}+\frac{\hbar}{4eBl_{\phi,2D}^2}\right] - \ln\left[\frac{\hbar}{4eBl_e^2}\right]}. \quad (4)$$

The magnetic-field range over which the fits were performed was $|B| \leq 20$ mT, to remain in the range of validity $l_e < l_B$ of the theoretical expressions. Fit parameters were α, W, and l_ϕ or $l_{\phi,1D}$ and $l_{\phi,2D}$. For the first series of fits, L was set to 800 nm. The quality of these fits, as expressed by the mean-square deviation χ^2 was comparable for all three formulas. Table I shows this for one of the curves from Fig. 3. However, for the 1D formula the fit result for W is always much larger than the gap in the split gate, and therefore not realistic. Although for the specific example in Table I the difference is only marginal, the 2D formula generally leads to values of W smaller than l_ϕ. This would mean that the sample is 1D instead of 2D. Only the fits according to Eq. (3) give realistic values for all parameters. The conclusion is that we cannot neglect the influence of the large 2D probes on the LFMC of the short 1D channel.

Figure 4 shows $l_{\phi,1D}$ and $l_{\phi,2D}$ as obtained from fits of Eq. (3) to all LFMC curves in Fig. 3. Fit parameters were L, W, α, $l_{\phi,1D}$, and $l_{\phi,2D}$. An additional condition in the fit procedure was $L > 730$ nm. After the initial fits were performed the fitted values for L, W, and α were averaged, and kept fixed during the final fits: $\langle L \rangle = 845 \pm 40$ nm, $\langle W \rangle = 120 \pm 20$ nm, and $\langle \alpha \rangle = 0.53 \pm 0.05$. $\langle L \rangle$ and $\langle W \rangle$ have quite reasonable values if the effect of fringing fields is taken into account. The value of α corresponds well to previous results for Si MOSFET's.[8]

If instead of a negative a *positive* voltage is applied to the split gate, the ratio between V_{GL} and V_{GU} can be chosen such that a homogeneous two-dimensional electron gas (2DEG) is present between the source and drain. For $V_{GU} = 15$ V this is the case if $V_{GL} = 6.92$ V. In this mode of operation $l_{\phi,2D}$ can be determined independent-

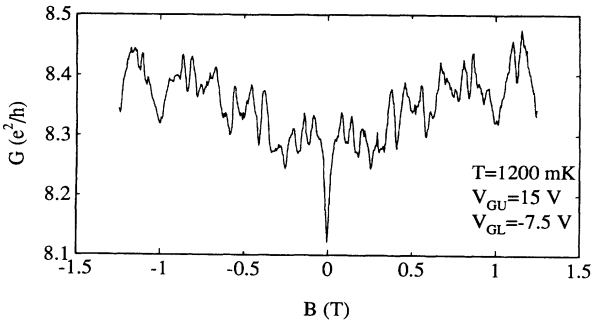

FIG. 2. Typical magnetoconductance curve for device No. 1.

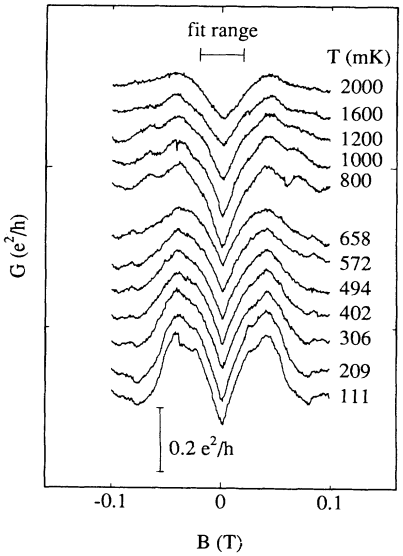

FIG. 3. Low-field magnetoconductance of device No. 1 at several temperatures between 0.1 and 2.0 K. $V_{GU} = 15$ V and $V_{GL} = -7.5$ V. Curves have been offset.

TABLE I. Fit results for the experimental curve at 402 mK in Fig. 3. The three columns are for the standard 1D weak-localization formula, the standard 2D formula, and Chandrasekhar's formula, respectively.

Weak-localization formula	1D [Eq. (1)]	2D [Eq. (2)]	1D-2D [Eq. (3)]
$\chi^2\times(10^{-4})$	3.1	1.7	2.0
W (nm)	1600	330	90
l_ϕ (nm)	90	360	
$l_{\phi,1D}$ (nm)			630
$l_{\phi,2D}$ (nm)			900

ly, by fits of the standard 2D expression (2) to the LFMC curves of the homogeneous 2DEG. Figure 4 also shows the results for these experiments. The values of $l_{\phi,2D}$ as determined from the curves in Fig. 3 agree very well with the independent results for the homogeneous electron gas. This, as well as the temperature dependence of $l_{\phi,2D}$ and $l_{\phi,1D}$ (which is discussed in the next part of this paper), gives great confidence in the quality of the fits of Eq. (3) to the data of Fig. 3. Because of the relatively large amplitude of the universal conductance fluctuations (see Fig. 2), these good results could not be expected *a priori*.

The temperature dependence of l_ϕ is determined by the dominant mechanism for phase breaking. At low temperatures electron-electron interaction is the dominant inelastic mechanism.[9] If these interactions involve large energy transfers,[10] they lead to a temperature-dependent phase-coherence length $l_\phi \propto T^{-d/4}$, with d the dimensionality of the system. The dimensionality is in this case determined by the magnitude of the thermal length $l_T=(\hbar D/kT)^{1/2}$ relative to the width of the system. For

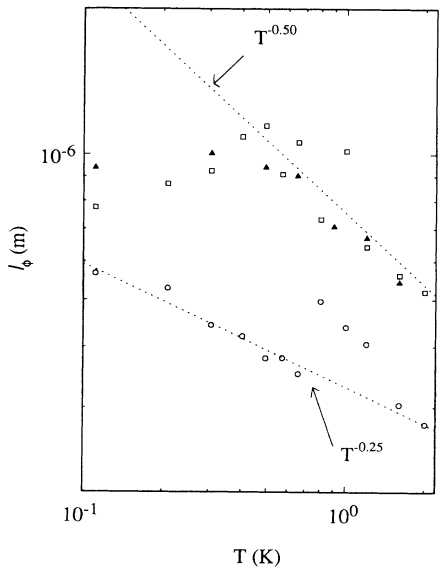

FIG. 4. Phase-coherence length as a function of temperature. Triangles indicate $l_{\phi,2D}$ as determined for the homogeneous 2D electron gas ($V_{GU}=15$ V, $V_{GL}=6.92$ V). Squares correspond to the fit results for $l_{\phi,2D}$, which were obtained from fits of Eq. (3) to the curves in Fig. 3 ($V_{GU}=15$ V, $V_{GL}=-7.5$ V). Circles are for $l_{\phi,1D}$. The slopes of the dashed lines correspond to $l_\phi \propto T^{-0.25}$ and $l_\phi \propto T^{-0.50}$.

low-dimensional systems ($d \leq 2$), quasielastic electron-electron interactions equivalent to a Nyquist mechanism[10,11] can also contribute significantly to the phase-breaking process. If the Nyquist mechanism dominates, the temperature dependence is given by $l_\phi \propto T^{1/(4-d)}$. For the fit results in Fig. 4 we find $l_{\phi,1D}=(330\pm10)(T/1\text{ K})^{-0.25\pm0.02}$ nm and $l_{\phi,2D}=(760\pm35)(T/1\text{ K})^{-0.50\pm0.09}$ nm in the high-temperature region where $l_{\phi,2D}$ has not yet saturated. In the fit of $l_{\phi,1D}$ the three strongly deviating points between $T=800$ mK and $T=1.2$ K were not included. Saturation of the phase-breaking length at low temperatures indicates that some temperature-independent phase-breaking mechanism becomes dominant at low temperatures. In our case phase breaking by rf radiation can be the origin, since only relatively weak rf-filtering was applied at the entrance of the cryostat.

For a 2D system both types of electron-electron scattering mentioned above predict an exponent -0.5 for the temperature dependence of l_ϕ. The experimentally found exponent -0.50 ± 0.09 for $l_{\phi,2D}$ corresponds well to these predictions. In a 1D system it is possible to distinguish between the two phase-breaking mechanisms. The experimental exponent of $l_{\phi,1D}(-0.25\pm0.02)$ is closest to the theoretical prediction for large energy-transfer electron-electron scattering. To check whether the narrow channel in the MOSFET is indeed 1D with respect to electron-electron scattering, we calculate l_T in the investigated temperature range. The 2D diffusion constant $D=(L/W)G/e^2N_{2D}$, where N_{2D} is the density of states, is estimated to be 8×10^{-3} m^2/s. Thus, $l_T\approx740$–170 nm in the temperature range between 111 and 2000 mK, and the channel operates in the one-dimensional regime. Since large energy transfer electron-electron scattering is the dominant inelastic mechanism in the 1D channel, this is probably also the case in the 2D regions.

Apart from the exponents, the magnitude of $l_{\phi,1D}$ and $l_{\phi,2D}$ has also been predicted theoretically[12,13] for the case of large energy-transfer electron-electron scattering:

$$l_{\phi,1D}=\left[\frac{\pi W N_{2D}\hbar D}{a\sqrt{2}}l_T\right]^{1/2}, \tag{5}$$

$$l_{\phi,2D}=\left[\frac{4\pi N_{2D}\hbar D}{a}l_T^2\right]^{1/2}. \tag{6}$$

Here, the parameter a has a theoretical value of 1 at zero temperature. Using these formulas under the assumption that the diffusion constant and density of states for the 1D and 2D areas of the MOSFET are equal, we find $l_{\phi,1D}/l_{\phi,2D}=(W/4\sqrt{2}l_T)^{1/2}=0.29$ at 1 K. The experimental value $l_{\phi,1D}/l_{\phi,2D}=0.43\pm0.04$ (at 1 K) lies in the proper range when compared with the theoretical value.

A similar fit procedure has been applied to the LFMC curves for device No. 2. Apart from the quite different value of $\langle L\rangle$, because of the shorter split gate, the results are comparable to those for device No. 1: $\langle L\rangle=280\pm80$ nm, $\langle W\rangle=85\pm20$ nm, $\langle\alpha\rangle=0.58\pm0.05$, $l_{\phi,1D}\propto(250\pm50)(T/1\text{ K})^{-0.2\pm0.1}$, and $l_{\phi,2D}\propto(660\pm20)(T/1\text{ K})^{-0.5\pm0.1}$. For this device the temperature depen-

dence of $l_{\phi,1D}$ and $l_{\phi,2D}$ also indicates that large energy-transfer electron-electron scattering is the dominant phase-breaking mechanism. However, the quality of the fits is much less than for device No. 1 and for some temperatures no acceptable fit of Eq. (3) to the data could be obtained. A possible reason for this difference is that for device No. 2 $\langle L \rangle$ is not much larger than l_e. Transport through the 1D channel is then not really diffusive, and can deviate from the predictions of weak-localization theory. Therefore, for semiconductors, in which l_e is usually long when compared with metals, the limits of applicability of Eq. (3) will be reached for relatively long 1D channels. Another reason for the relatively low quality of the fits for device No. 2 could be that universal conductance fluctuations play a more important role than in device No. 1, thus obscuring the weak-localization behavior around zero field.

In summary, we experimentally determined the low-field magnetoconductance of short 1D wires contacted by 2D probes in Si MOSFET's, and showed that a recent extension of the weak-localization theory by Chandrasekhar *et al.*,[4,6] which includes the influence of probes, describes our data very well. From the temperature dependence of the phase-coherence length we found that in the investigated temperature range electron-electron scattering involving large energy transfers is the dominant phase-breaking mechanism. This is true both for the one-dimensional channel and for the two-dimensional probes.

This work is part of the research program of the "Stichting voor Fundamenteel Onderzoek der Materie," which is financially supported by the "Nederlandse Organisatie voor Wetenschappelijk Onderzoek."

---

*Present address: Philips Research Laboratories, 5600 JA Eindhoven, The Netherlands.

[1]B. L. Al'tshuler and A. G. Aronov, Pis'ma Zh. Eksp. Teor. Fiz. **33**, 515 (1981) [JETP Lett. **33**, 499 (1981)].

[2]S. Hikami, A. I. Larkin, and Y. Nagaoka, Prog. Theor. Phys. **63**, 707 (1980).

[3]P. A. Lee and T. V. Ramakrishnan, Rev. Mod. Phys. **57**, 289 (1985).

[4]V. Chandrasekhar, P. Santhanam, and D. E. Prober, Phys. Rev. Lett. **61**, 2253 (1988).

[5]D. E. Khmel'nitskii, Physica **126B**, 235 (1984).

[6]V. Chandrasekhar, P. Santhanam, and D. E. Prober, Phys. Rev. B **44**, 11 203 (1991).

[7]A. H. Verbruggen, H. Vloeberghs, P. A. M. Holweg, C. Van Haesendonck, S. Radelaar, and Y. Bruynseraede, Phys. Rev. B **45**, 8799 (1992).

[8]H. Fukuyama, Surf. Sci. **113**, 489 (1982); J. R. Gao, C. de Graaf, A. S. Schüssler, J. Caro, S. Radelaar, and K. Heyers, Phys. Rev. B (to be published).

[9]H. Fukuyama and E. Abrahams, Phys. Rev. B **27**, 5976 (1983).

[10]B. L. Al'tshuler and A. G. Aronov, in *Electron-Electron Interactions in Disordered Systems*, edited by A. L. Efros and M. Pollak (North-Holland, Amsterdam, 1985).

[11]B. L. Al'tshuler, A. G. Aronov, and D. E. Khmel'nitskii, J. Phys. C **15**, 7367 (1982).

[12]E. Abrahams, P. W. Anderson, P. A. Lee, and T. V. Ramakrishnan, Phys. Rev. B **24**, 6783 (1981).

[13]R. G. Wheeler, K. K. Choi, A. Goel, R. Wisnieff, and D. E. Prober, Phys. Rev. Lett. **49**, 1674 (1982).